Archives of Environmental Protection
Vol. 50 no. 3 pp. 109–121

PL ISSN 2083-4772
DOI:10.24425/aep.2024.151690

The improvement of Beijing ambient air quality resulting from the upgrade of vehicle emission standards

Chang Wang[1], Xiaohan Miao[1], Maodong Fang[2]*, Yuan Chen[1], Taosheng Jin[1]*

[1]Tianjin Key Laboratory of Urban Transport Emission Research, State Environmental Protection Key Laboratory of Urban Ambient Air Particulate Matter Pollution Prevention and Control, College of Environmental Science and Engineering, Nankai University, Tianjin, 300350, China
[2]National Engineering Laboratory for Mobile Source Emission Control Technology, China Automotive Technology and Research Center Co., Ltd., Tianjin 300300, China

* Corresponding author's e-mail: jints@nankai.edu.cn, fangmaodong@catarc.ac.cn

Keywords: emission standards; response surface model (RSM); environmental improvement; ozone (O_3); particulate matter (PM)

Abstract: To investigate the effects and improvements of tightening vehicle emission standards from China III to China V on ozone (O_3) and particulate matter (PM) pollution in the atmospheric environment, this study obtained emission factors of O_3 and PM precursors such as nitrogen oxides (NOx), volatile organic compounds (VOCs), and primary PM from gasoline and diesel vehicles through actual testing. Response surface models (RSM) were then created for the environmental concentrations of the target pollutants O_3 (RSM-O_3_HSS6-200) and PM (RSM-PM_HSS9-300) as functions of precursor pollutant emissions. Beijing was chosen as the main receptor region, with the China III emission standard serving as the baseline scenario and the China IV and V standards as control scenarios. The results indicate that as vehicle emission standards tightened from China III to China IV and V, O_3 concentrations in Beijing's environment decreased from 92.7 ppbv to 78.47 ppbv and 72.20 ppbv, respectively, while PM concentrations decreased from 64.12 μg/m³ to 48.23 μg/m³ and 38.60 μg/m³, respectively. Furthermore, the environmental benefits achieved from China III to China IV were higher than those from China IV to China V. Additionally, an analysis of pollutant source contributions revealed that NOx played a major role in reducing O_3 concentrations, while primary PM was crucial in controlling PM pollution.

Introduction

In recent years, the air quality issues caused by surface ozone (O_3) and PM in Beijing-Tianjin-Hebei region, especially in Beijing, China, have attracted significant attention from governments at all levels and the general public. Surface O_3 is a secondary pollutant produced by photochemical reactions involving nitrogen oxides (NOx) and volatile organic compounds (VOCs). PM is a complex mixture consisting of primary PM, which comes directly from emission sources, and secondary aerosol components formed through atmospheric chemical reactions involving pollutants like NOx, VOCs, NH_3 and SO_2 (Liu et al., 2008; Xue, 2000).Specifically, NOx can decompose into oxygen atoms under sunlight, which then react with atmospheric oxygen to create O_3. VOCs can also be broken down into smaller organic molecules and free radicals under sunlight, which perpetuates O_3 formation (Liu et al., 2021). Additionally, some chemical reactions among NOx, VOCs, NH_3 and SO_2 can generate some low volatile compounds, which can then condense onto primary PM or among themselves to form new PM (Nguyen et al., 2002).

The formation of surface O_3 and PM can adversely affect human health,and motor vehicle emissions are one of the primary sources of these pollutants (Zhang et al., 2023; Kumar et al., 2021). According to the latest pollutant emission inventory, NOx emissions from vehicles account for over 80% of mobile sources in Beijing, while VOC emissions from vehicles constitute approximately 30% (Xu et al., 2020). Based on recent analyses of fine $PM_{2.5}$ sources in Beijing, vehicle pollution contributes to 45% of local emissions (PGBM, 2021; Daellenbach et al., 2020). In addition to the directly emitted $PM_{2.5}$, the contribution of their secondary formation also deserves attention.

In China, the continuous increase in car ownership and congestion during morning and evening peak hours contribute to the increasing severity of traffic pollution. In 2021, the number of vehicles in China reached 395 million, a 6.2% increase compared to the same period in 2020. There are seventy-nine cities in China with over one million vehicles, with Beijing being the only city with more than six million gasoline vehicles. Gasoline vehicles dominate urban road fleets, while diesel vehicles remain the primary carrier of

intercity freight transportation (MEE, 2022). According to statistics, the total vehicle emissions of NOx, VOCs, and $PM_{2.5}$ in China could reach 5.26 million tons, 1.91 million tons and 53 thousand tons, respectively, in 2022 (MEE, 2023; Guha et al., 2023).

Therefore, further research to strengthen the control of vehicle pollution is necessary for improving ambient air quality and safeguarding public health. China has continuously upgraded fuel and vehicle emission standards to reduce the emissions of O_3 and PM precursor, as well as other pollutants emitted by vehicles (Lyu et al., 2020). Nevertheless, there remains a considerable gap between the expected effects of policy implementation and environmental protection requirements, despite the government's efforts to improve air quality (Wang et al., 2020). Environmental governance in China has reached a critical stage, where precise treatment of pivotal environmental problems is necessary to control emissions and achieve clear goals.

The implementation of fuel and vehicle emission standards in China follows a phased approach: Beijing precedes the Beijing-Tianjin-Heibei (BTH) region, and the BTH region precedes the rest of China. Therefore, analyzing the relationship between upgrading of vehicle emission standards upgrade and ambient O_3 and PM levels in Beijing is crucial for promoting policies and achieving national unification of standards. Based on vehicle emission tests, this study used Response Surface Methodology (RSM) and Response Surface Modeling-Visualization & Analysis Tool (RSM-VAT) to analyze the degree of O_3 and PM concentration reduction during the upgrade of vehicle emission standards from China III to China V. The study demonstrates the contribution of current control measures to the reduction of vehicle emission pollutants and related environmental problems. The findings of this study have the potential to aid the government in formulating effective strategies for future emission abatement.

Methodology

Research content and scheme

In this study, vehicle emission experiments were conducted on light-duty gasoline vehicles and heavy-duty diesel vehicles to obtain vehicle emission factors for several typical pollutants, such as NOx, VOCs, and primary PM. Additionally, background data, including the geographic zones of the study object, were collected to form a data file that met the model format requirements for analysis. These data files were used as input for the RSM for subsequent simulation evaluation of pollutant concentrations in corresponding regions. The RSM was developed by designing control scenarios, sample statistics, numerical simulations, and reliability testing, which established a functional relationship between source-specific emissions and air pollution conditions. This enabled a rapid response of the ambient concentration of the target pollutant under the specified emission scenario. Changes in O_3 and PM concentrations and regional distributions in Beijing could be output through RSM, and then, using RSM-VAT developed by Lao et al., (2012), to evaluate the environmental improvement resulting from the upgrade of vehicle emission standards in Beijing.

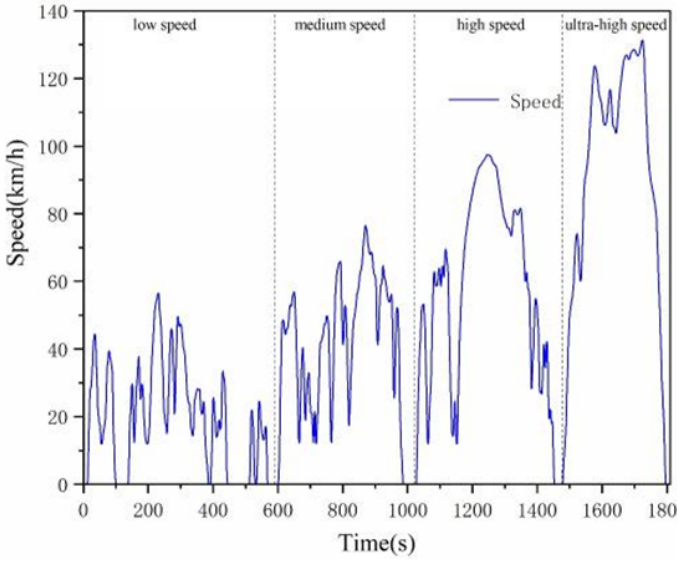

Figure S1. The speed-time relation curve in WLTC

Emission test

As shown in Figure S1, the test cycle was the World Light Vehicle Test Cycle (WLTC), which includes four parts: low speed, medium speed, high speed, and ultra-high speed. The total cycle duration was 23.266 km, with a maximum cycle driving speed of 131.8km/h.

The light vehicle emission test system mainly included a chassis dynamometer, particulate matter counter, and a full flow dilution sampling and analysis system for sampling and measuring exhaust pollutants. The test vehicles were immersed in the designated immersion area for 6h-36h to ensure that the engine oil temperature and coolant temperature were maintained at 23±2°C before the start of the test.

Exhaust pollutants (CO, NOx, VOCs, etc.) were measured using a CFV-CVS (Critical Flow Venturitube-Constant Volume Sampling) system. CO was analyzed by the non-spectroscopic infrared method, VOCs by flame ionization detection, and NOx by the chemiluminescence method. Exhaust pollutants collected during each stage of the WLTC were sampled after dilution. Subsequently, the emissions of each pollutant were analyzed and calculated.

Based on the data gathered from various speed segments, the emissions of gaseous pollutants across distinct speed ranges were computed:

$$M_{i,phase}=\frac{V_{mix,phase}\times\rho_i\times k_{H,phase}\times C_{i,phase}\times 10^{-6}}{d_{phase}} \quad (1)$$

In the equation, denotes the measured quantity (g/km) of the i-th pollutant; is the volume (L/experiment) of dilution gas corrected to standard conditions (273.15K and 101.325 kPa); is the density (g/L) of the i-th pollutant at standard temperature and atmospheric pressure; is the humidity correction factor for pollutant emissions; is the concentration v/v (vppm); and is the driving distance (km) of the chassis dynamometer test.

The calculation formula for determining the value of is as follows:

$$C_i=C_e-C_d\times\left(1-\frac{1}{DF}\right) \quad (2)$$

In the equation, is the volume fraction (vppm) of the i-th pollutant in the dilution gas measurements; is the volume fraction (vppm) of the i-th pollutant in the dilution air measurements; and *DF* denotes as the dilution factor.

For gasoline, the following formula is used to calculate the dilution factor:

$$DF=\frac{13.4}{C_{CO_2}+（C_{VOCs}+C_{CO}）\times 10^{-4}} \quad (3)$$

For gasoline, the following formula is used to calculate the humidity correction factor:

$$k_H=\frac{1}{1-0.0329\times（H-10.71）} \quad (4)$$

$$H=\frac{6.211\times R_a\times P_d}{P_B-P_d\times R_a\times 10^{-2}} \quad (5)$$

In the equation, is the absolute humidity, i.e., the mass of water vapor per unit mass of dry air (g/kg); is the relative humidity (%) of the ambient air during the test; is the saturation vapor pressure (kPa) at the ambient temperature during the test; and is the current atmospheric pressure (kPa) in the test cell. The factor should be calculated separately for each speed segment in the test cycle, with the ambient temperature and relative humidity averaged over the continuous measurements during the respective speed segment.

Model stimulation

RSM involves analyzing and establishing a specific functional relationship between the target response variable and each control factor through a particular scale and number of experimental designs, using mathematical statistics (Box and Draper, 2007). Applying RSM in air pollution research involves summarizing the expected environmental concentrations and the specific mathematical relationship between emissions of target pollutants and all source pollution factors through experimental methods and statistical means, aided by specific algorithm programs. The RSM model helps establish a rapid response and mapping relationship from pollution source emissions to pollutant concentrations. It can be used for rapid assessment of the outcomes of specific emission scenarios, such as emission reduction measures and related policy implementation effects.

Model design

The establishment of the RSM model relies on determining the relationship between controllable source emissions and pollution levels through a response function. The process of building an RSM model involves five steps: selecting and determining control factors, designing control scenarios, selecting reasonable experimental parameters, fitting response (function) relationships, and verifying model reliability.

(1) Selection of Control Factors

Control factors refer to emission parameters. Selecting appropriate control factors based on research needs is a prerequisite for control matrix design in RSM construction. Generally, starting from the research objective, various relevant pollutants from different regions and sources that are related to the target range are determined as emission control factors.

In this study on O_3 and PM pollution in the Beijing region, the selected control factors include NOx emissions from light gasoline vehicles, NOx emissions from heavy diesel vehicles, other NOx emissions, VOC emissions from light gasoline vehicles, VOC emissions from heavy diesel vehicles, and other VOC emissions.

(2) Design of Control Scenario

Control scenarios correspond to changes in control factor coefficients. To generate a sampling space for studying control factors, samples are collected to characterize the changes in the corresponding control factor(s). Achieving the highest sampling efficiency and saving time and computational costs in model construction is the key element of the sampling process. Effective and fast sampling methods are required to achieve this goal. The Latin Hypercube Sampling (LHS) method can make the obtained samples distributed relatively uniformly in the global sampling space and reflect actual situations more realistically. However, it has some problems, as the results of each random sample can differ significantly (Box and Draper, 2007; Hammersley, 1960).

To improve the stability of experiments and simulations, some researchers have used a more reliable sampling method, the Hammersley Quasi-Random Sequence Sample (HSS) (Hammersley, 1960), implemented through specific program algorithms. HSS ensures both the uniform distribution of sampling results in the space and the credibility of the results, thereby improving the reproducibility of sampling. Therefore, HSS is increasingly applied in RSM for sample generation and control scenario construction. This study employed a two-dimensional uniform sampling method for the control factors utilizing the HHS.

(3) Selecting experimental parameters

In the RSM model, selecting an appropriate number of samples is a crucial step for successful model construction. Xing Jia designed an analysis method using simulation experiments to determine the minimum required sample size for experiments with a given number of control factors by constructing a “virtual response” relationship (Xing, 2011). Based on previous research experience, two RSM models created in this study selected 200 (RSM-O_3) and 300 (RSM-PM) samples respectively to ensure the reliability and accuracy of simulation results.

(4) Nonlinear statistics (response relationship fitting)

After determining the control factors and experimental parameters, samples are generated through computational simulation and nonlinear mathematical statistical analysis. Early response RSM models used the MPerK program for model construction, combined with Kriging interpolation, and utilized maximum likelihood estimation methods (Zhao et al., 2013a). Currently, polynomial fitting techniques based on chemical mechanisms are used instead of the original black-box statistical methods to elucidate the essential response relationship between characteristic pollutant concentrations and source emissions. These techniques quickly extract and quantify the nonlinear features of different species’ responses to environmental concentrations (Jia et al., 2017; Zhao et al., 2013b).

Reliability verification

In completed research, the reliability of RSM prediction results is mainly verified using three methods: "External Verification", "Leave-One-Out Cross-Validation (LOO-CV)", and "Pairwise Isoline Verification (PIV)". External validation is the most commonly used method, which tests the entire RSM model by adding external validation samples. This method can evaluate the reliability of the constructed RSM system under a specific control scenario. LOO-CV involves partitioning the data sample into numerous smaller subsets, where each iteration excludes one sample for evaluation while the remaining samples serve primarily to evaluate the stability of the entire statistical simulation system (Aelion et al., 2009). PIV is used to evaluate the reliability and stability of RSM within different dimensions and the entire spatial range.

The advantage of LOO-CV is that the test can be performed within the range of the experimental fitted sample, and it does not require time to prepare new simulation scenarios. However, the disadvantage of this method is that it cannot investigate the stability of an RSM model constructed outside the experimental sample range. For external validation, the number of scenarios introduced is limited due to the long time required for model simulation. Compared to LOO-CV, external validation can analyze the accuracy and reliability of RSM's prediction results for the research target under specified control scenarios beyond the scope of the research sample, making it the most important method for reliability testing. Therefore, this study employed external validation to assess the reliability of the constructed RSM models based on the external validation function module provided by RSM-VAT.

Software flow

RSM-VAT comprises three modules: RSM Modeling Experimental Design (Experimental Design), Data Validation (QA & Validation), and Data Visualization & Analysis (Visualization & Analysis). Each subsystem plays a unique functional role in constructing RSM and generating analysis results. Figure S2 visually presents the functional framework of RSM-VAT. The RSM building block first establishes the response surface model (RSM) and generates a series of policy files based on relevant input parameters, which provide input files for subsequent steps. After the RSM is constructed, the Data Validation module checks whether the prediction error of the established RSM system is within an acceptable range. Upon confirming that the error is acceptable, the Visualisation & Analysis module displays the response relationship between controlling pollutant emissions and predicting environmental concentrations, and analyzes and outputs a series of related characteristic laws.

Results and discussion

Emission factors of vehicle

The data on NOx, VOCs, and primary PM emissions from light-duty gasoline vehicles and heavy-duty diesel vehicles under China III to China V emission standards were collected and summarized in Table 1. By normalizing the relevant pollutant emission factors to corresponding emission standards, the corresponding control coefficients were obtained and are presented in Table 2.

Model performance

Using RSM-VAT 2.6, this study constructed the O_3-RSM model (RSM-O_3) and the PM-RSM model (RSM-PM) for the Beijing region, establishing the response relationship between the concentration of O_3 and PM and the emissions of each precursor pollutant. Through control scenario analysis of the two target pollutants, the environmental concentrations of O_3 and PM in the Beijing region during the period of the China III to China V emission standards were studied. The response of

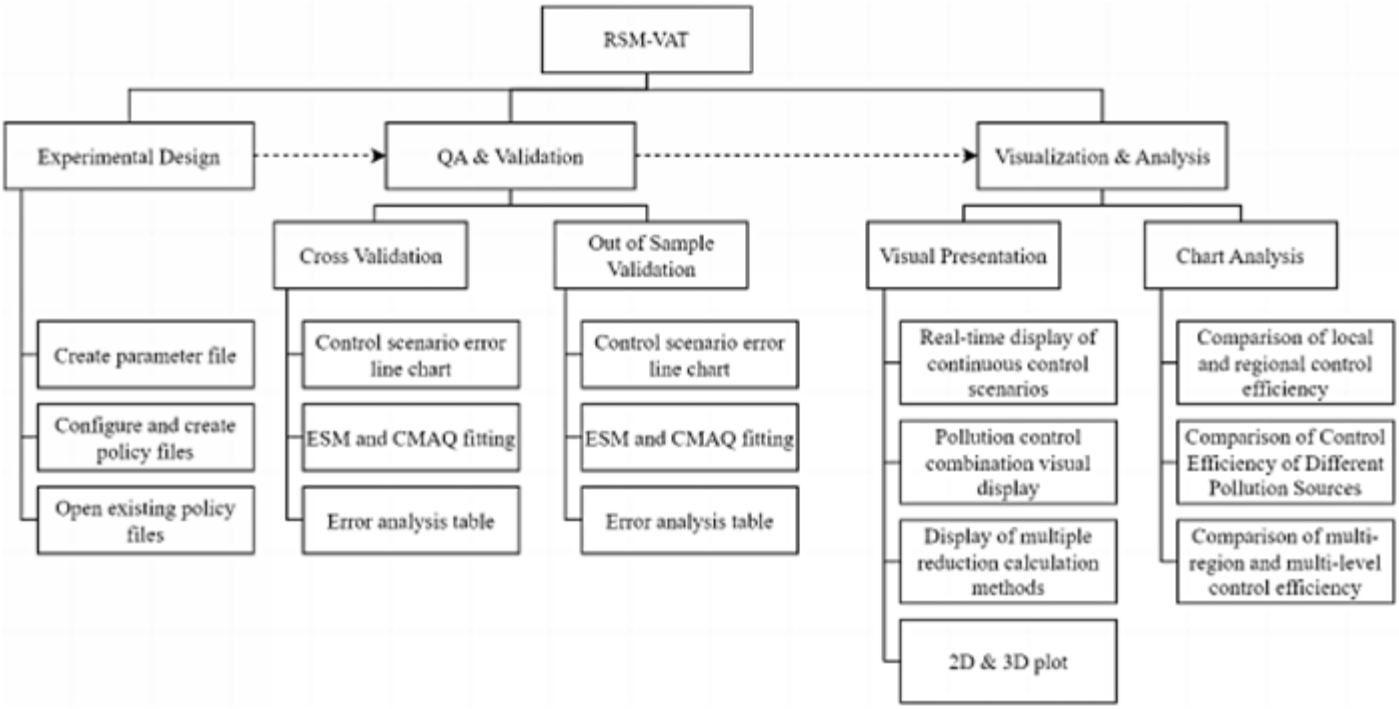

Figure S2. RSM-VAT functional structure

Table 1. Vehicle emission factors under China III to China V emission standards

Emission standards		NO_x (mg/km)	VOCs (mg/km)	PM (mg/km)
Light gasoline vehicles	China III	206.42	233.12	6.00
	China IV	88.53	84.98	3.60
	China V	27.88	42.88	1.91
Heavy diesel vehicles	China III	7976.71	811.95	63.77
	China IV	5224.06	516.77	33.22
	China V	4846.96	472.77	14.42

Table 2. Control coefficient of vehicle emission factors in different emission scenarios

Emission standards		NO_x (mg/km)	VOCs (mg/km)	PM (mg/km)
Gasoline vehicle	China III	1	1	1
	China IV	0.43	0.36	0.6
	China V	0.14	0.18	0.32
Diesel vehicle	China III	1	1	1
	China IV	0.65	0.63	0.52
	China V	0.61	0.59	0.22

O_3 and PM pollution to the evolution of emissions standards from China III to China V was also analyzed to assess the environmental improvements resulting from stricter emission standards for vehicles. In addition, external verification methods were used to test the reliability of the RSM system and ensure the accuracy of the established RSM models in predicting the environmental concentration of target pollutants.

Model Construction

(1) O_3

A response surface model (RSM) was used to analyze the nonlinear relationship between O_3 ambient concentration and two precursor pollutants, NOx and VOCs. The control factors were divided into six types based on the research purpose: NOx emissions from light gasoline vehicles, NOx emissions from heavy diesel vehicles, NOx emissions from others, VOC emissions from light gasoline vehicles, VOC emissions from heavy diesel vehicles, and VOC emissions from others. Two-dimensional uniform sampling of the control factors was carried out using HHS with 20 samples. The resulting response surface model is called RSM-O_3_HSS6-200.

(2) PM

In a similar manner to the O_3-RSM modeling process, this study selected three controllable precursor pollutants - NOx, VOCs and PM - as control factors, while NH_3 and SO_2 were kept unchanged. The three control factor species were divided into nine types based on research needs, which included NOx and VOC emissions from light-duty gasoline vehicles, heavy-duty diesel vehicles, and other sources, as well as PM emissions from light-duty gasoline vehicles, heavy-duty diesel vehicles, and other sources. The same sampling method was applied to 300 samples, and the resulting response surface model, called RSM-PM_HSS9-300, was established.

Reliability analysis

(1) O_3

The external testing results of the RSM-O_3_HSS6-20 are presented in Table 3, with the mean bias (MB) and mean error (ME) of RSM prediction results being 1.68×10^{-18} μg/m^3 and 1.83×10^{-18} μg/m^3, respectively. The mean normalized bias (MNB) and mean fractional bias (MFB) were 2.22×10^{-19} %, while the mean normalized error (MNE) and mean fractional error (MFE) were 2.66×10^{-19} %, with the maximum value of

Table 3. RSM-O_3 External verification error and bias

Index	External validation (Number of scenarios=20)		
	Mean	Maximum	Minimum
Mean bias/ (μg/m³)	1.68×10-18	1.88×10-17	-6.68×10-19
Mean error/ (μg/m³)	1.83×10-18	1.79×10-17	0
Mean normalized bias	2.22×10-19 %	2.55×10-18 %	-2.39×10-19 %
Mean normalized error	2.66×10-19 %	2.55×10-18 %	0
Mean fractional bias	2.22×10-19 %	2.55×10-18 %	-2.39×10-19 %
Mean fractional error	2.66×10-19 %	2.55×10-18 %	0

Table 4. RSM-PM External verification error and bias

Index	External validation (Number of scenarios=30)		
	Mean	Maximum	Minimum
Mean bias/ (μg/m³)	2.25×10-17	1.88×10-16	-8.88×10-18
Mean bias/ (μg/m³)	2.33×10-17	1.79×10-16	0
Mean standard bias	1.22×10-18 %	1.65×10-17 %	-3.36×10-18 %
Mean standard error	1.69×10-18 %	1.65×10-17 %	0
Mean fractional bias	1.22×10-18 %	1.65×10-17 %	-3.36×10-18 %
Mean fractional error	1.69×10-18 %	1.65×10-17 %	0

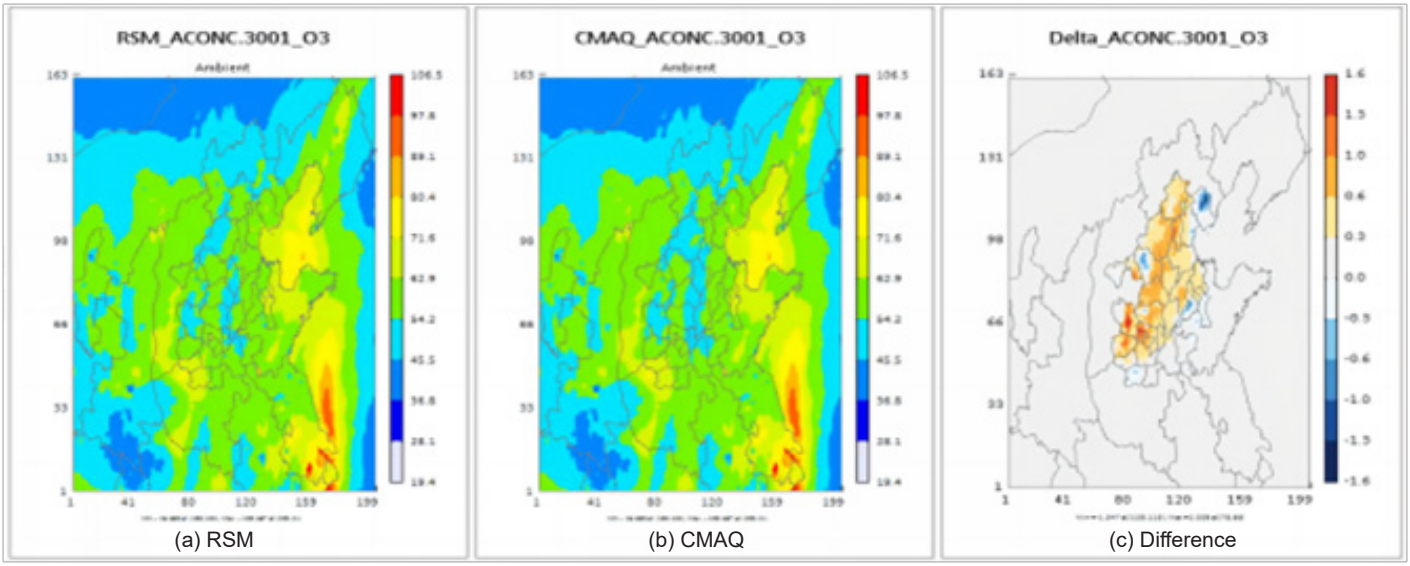

Figure 1. Two-dimensional plot comparing O_3 predictions for CMAQ and RSM

these four items being 2.55×10^{-18} %. These results indicate that the RSM-O_3_HSS6-200 model established by the institute has high reliability for predicting environmental O_3 concentration, with errors and deviations within acceptable ranges.

Figure 1 compares the average O_3 concentrations obtained from the RSM-O_3_HSS6-20 model under the external validation scenario ACONC.3001 with those from the CMAQ simulation. Specifically, Figures 1(a) and (b) depict the O_3 average concentration response diagrams simulated by RSM and CMAQ, respectively. Meanwhile, Figure 1(c), labeled as "Delta_ACONC.3001_O_3," illustrates the discrepancies between the RSM-O_3_HSS6-200 and CMAQ simulation outcomes.

The analysis reveals notable differences in O_3 concentrations predicted by RSM-O_3_HSS6-20 and the CMAQ simulations. However, it is worth noting that all absolute error values fall within 1.6 μg/m³. This finding underscores the reliability of the RSM-O_3 model developed in this study for predicting O_3 concentrations in the control scenario specific to the Beijing region. Therefore, the RSM-O_3_HSS6-20 model holds promise as a valuable tool to aid in environmental impact assessments related to vehicle emission standards upgrades.

Figure 2 presents the least squares linear regression lines for O_3 concentrations modeled by RSM and CMAQ under control scenarios ACONC.3001, ACONC.3002, ACONC.3003, and ACONC.3004. It is observed that all four regression lines closely overlap with the line of slope 1 (x:y=1:1). Specifically, the correlation coefficients (r) between the results obtained from RSM and CMAQ methods are greater than 0.999 for all four control scenarios, with values of 0.9997972, 0.9996918, 0.9997576, and 0.9998389, respectively.

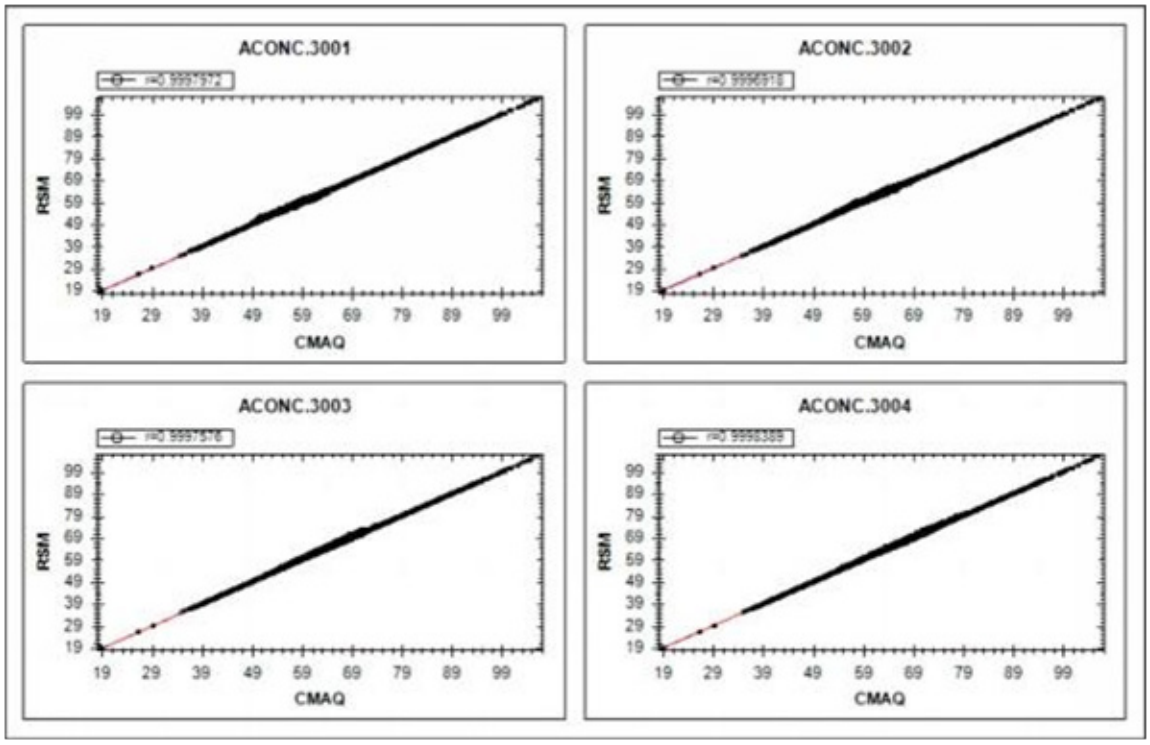

Figure 2. Distribution scatter plot comparing O_3 predictions for CMAQ and RSM

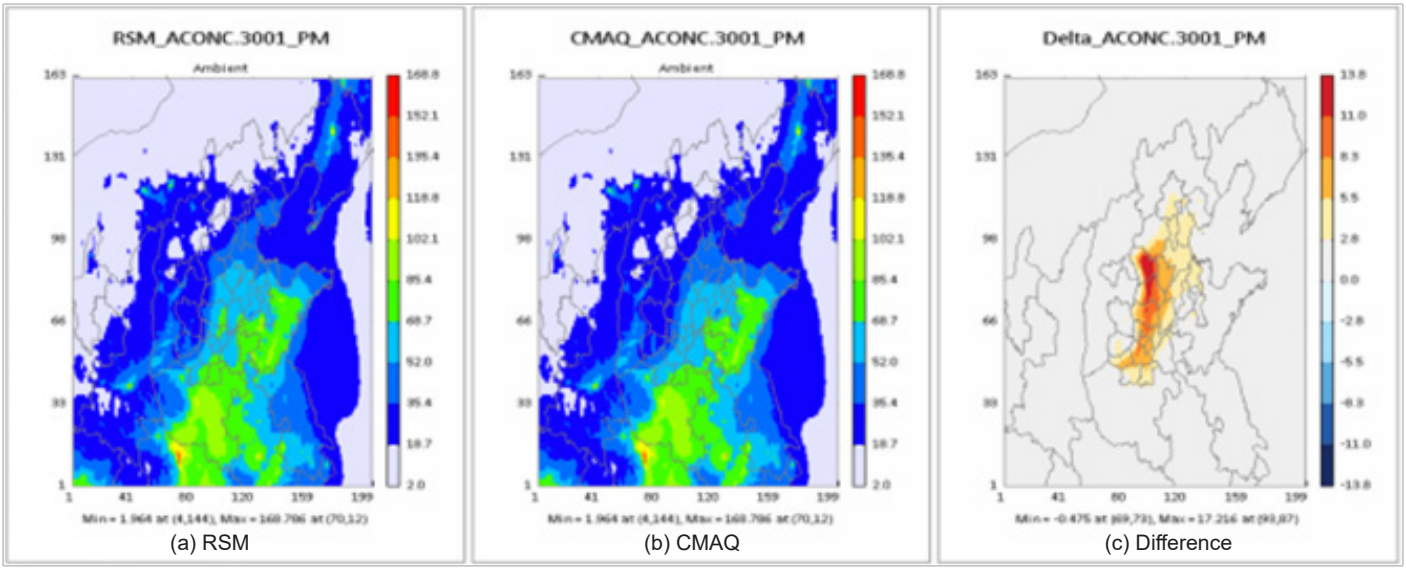

Figure 3. Two-dimensional plot comparing PM predictions for CMAQ and RSM

Overall, the RSM-O_3_HSS6-20 model is a reliable tool for predicting environmental O_3 concentrations and can be used for environmental impact assessments of vehicle emission standard upgrades.

(2) PM

The external testing results of the RSM-PM_HSS9-300 are presented in Table 4, with MB and ME of the simulated PM environmental concentration being 2.25×10^{-17} μg/m^3 and 2.33×10^{-17} μg/m^3, respectively. The values of MNB and MFB were 1.22×10^{-18} %, while the MNB and MFE values were both 1.69×10^{-18} %, with the maximum value of all four items being 1.65×10^{-17} %. These results indicate that the RSM-PM_HSS9-300 model has high accuracy and reliability for predicting PM environmental concentrations under the designed control scenario.

Figure 3 presents a comparison of average PM concentrations derived from the RSM-PM_HSS6-300 model under the external validation scenario ACONC.3001 against those obtained from the CMAQ simulation. Specifically, Figures 3 (a) and 3(b) focus on PM average concentration response diagrams simulated by RSM and CMAQ, respectively. Additionally, Figure 3 (c), designated as "Delta_ACONC.3001_PM," highlights the variations between the RSM-PM_HSS6-300 and CMAQ simulation results for PM.

The analysis reveals differences in PM concentrations predicted by the RSM-PM_HSS6-300 model compared to the CMAQ simulations. However, all absolute error values are within an acceptable range of 13.8 μg/m^3. Although this error margin is higher than that observed for O_3, it still falls within tolerable limits. Therefore, this finding reinforces the

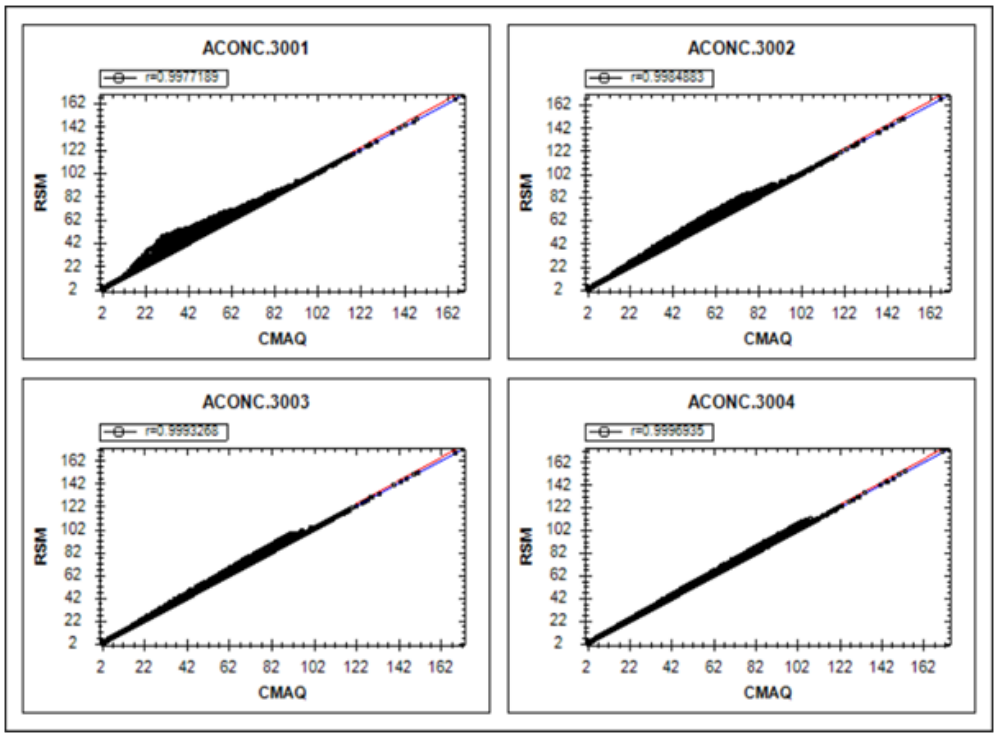

Figure 4. Distribution scatter plot comparing PM predictions for CMAQ and RSM

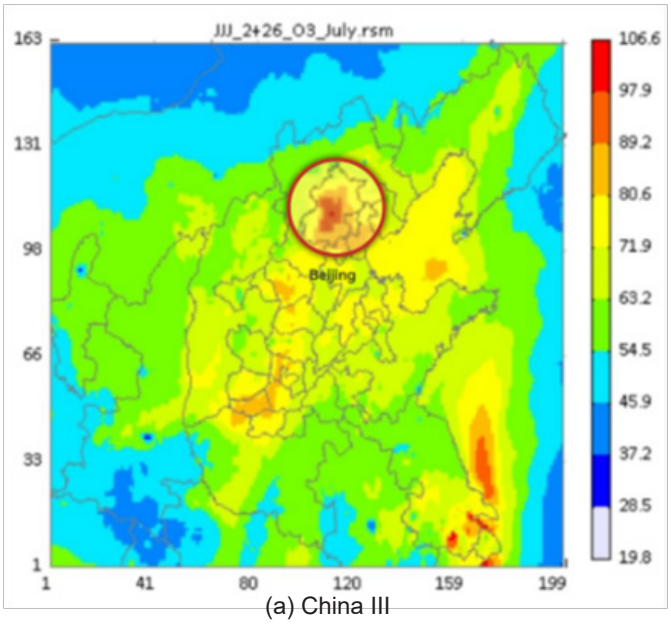

(a) China III

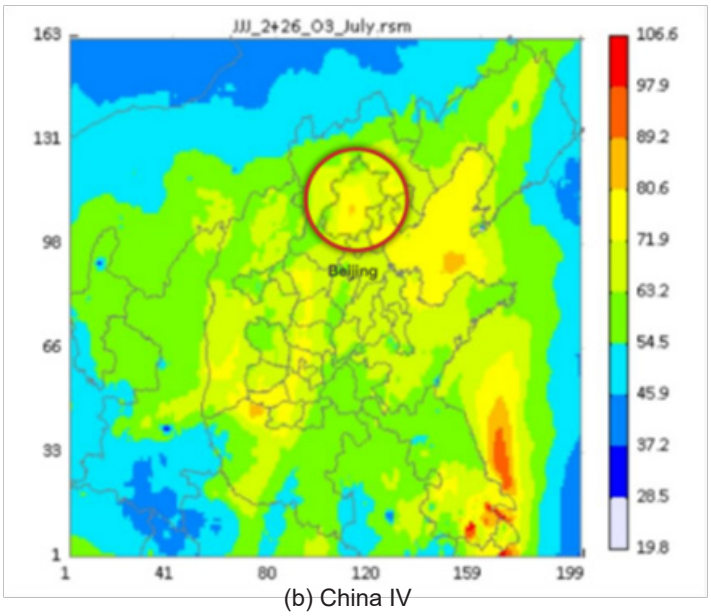

(b) China IV

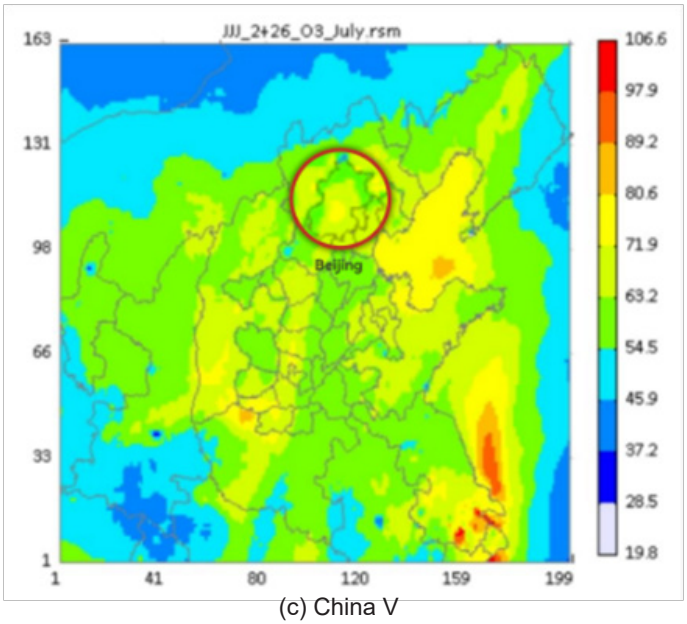

(c) China V

Figure 5. Two-dimensional distribution of O_3 concentration under different emission standard

reliability of the RSM-PM model developed in this study for predicting PM concentrations in the Beijing-specific control scenario. Consequently, the model holds promise as a valuable tool for supporting environmental impact assessments related to vehicle emission standards upgrades.

Figure 4 displays the least squares linear regression lines representing PM concentrations modeled by both RSM and CMAQ under four distinct control scenarios: ACONC.3001, ACONC.3002, ACONC.3003, and ACONC.3004. Notably, all four regression lines align closely with the diagonal line, suggesting a strong agreement between the modeling outcomes. Specifically, the correlation coefficients (r) between the RSM and CMAQ results exceed 0.999 for all control scenarios, with values of 0.9977189, 0.9984883, 0.9993268, and 0.9996935, respectively.

In conclusion, the RSM-PM_HSS6-300 model has proven to be a reliable tool for forecasting environmental PM concentrations, making it well-suited for conducting environmental impact assessments related to the enhancement of vehicle emission standards.

Analysis of RSM simulation results

(1) O_3

To analyze the environmental improvement of upgrading from China III to China V emission standards, the O_3 pollution conditions under the China III emission standards were set as the baseline scenario, while the China IV and V emission standards were set as the control scenarios. The RSM-O_3_HSS6-20 model was used to predict the O_3 ambient concentration in the receptor region (Beijing) under different scenarios. Additionally, RSM-VAT was used to generate the O_3 concentration distribution plot for the receptor area (Beijing) to illustrate the O_3 pollution status.

Figure 5 is a 2D plot showing the distribution of O_3 concentration, with a minimum of 19.8 μg/m^3 and a maximum of 106.6 μg/m^3.

It clearly shows that the O_3 ambient concentration in Beijing decreased significantly with the upgrade from the China III to China V emission standards and the resulting reduction in precursor pollutant emissions (NOx and VOCs). In addition, the decrease was more pronounced in areas with heavy O_3 pollution, indicating that these regions with higher O_3 ambient concentrations were more sensitive to changes in emission standards than other areas. The O_3 concentrations under the China III emission standard (baseline scenario) and the two control scenarios, China IV and China V, were 92.70 ppbv, 78.47 ppbv and 72.20 ppbv, respectively. This indicates that the progressively stringent emission standards from China III to China V have effectively controlled the emissions of O_3 precursor pollutants from vehicle exhaust, resulting in a significant direct decrease in the concentration of primary pollutants in the air. Consequently, this has indirectly led to a reduction in the ambient concentration of O_3 (a secondary pollutant).

However, in reality, O_3 pollution has not been effectively alleviated. Environmental monitoring data from the Beijing Ecology and Environment Bulletin (BMEEB) indicate that the annual average concentration of O_3 in Beijing was 99.78 μg/m^3 in 2014, 102.42 μg/m^3 in 2017, and 108.08 μg/m^3 in 2019. This discrepancy between actual monitoring concentrations

and model results can be attributed to the complexity of O_3 pollution sources and formation mechanisms. The influencing mechanisms of O_3 are significantly more complex in practice than theoretical models suggest, leading to an increase in O_3 concentration due to the combined effects of multiple factors.

Figure 6 shows the contribution of the two precursor pollutants (NOx and VOCs) to the reduction of O_3 concentration with the upgrade from the China III to the China IV and China V emission standards, as determined by the source distribution function of RSM-VAT. The O_3 concentration under the China III emission standard was set as the baseline scenario, while the China IV and V emission standards served as the control scenario. The results of the source contribution analysis indicate that both VOCs and NOx have a significant effect on O_3 pollution, with NOx playing the major role in reducing O_3 concentration under the upgraded emission standards from China III to China V. This is closely related to the concentration of vehicle emission pollutants (NOx and VOCs), as well as the complex atmospheric chemical processes and control mechanisms of O_3 formation (Latha et al., 2023).

(2) PM

To assess the environmental enhancement resulting from the transition from the China III to China V emission standards, the study established a baseline scenario representing PM pollution conditions under the China III standards. In contrast, the control scenario encompassed the China IV and V emission standards. Utilizing the RSM-PM_HSS6-300 model, predictions were made regarding particulate matter (PM) ambient concentrations in the target region of Beijing for these distinct scenarios. Furthermore, the RSM-VAT tool was employed to generate a visual representation of the PM concentration distribution in Beijing, providing a comprehensive overview of the PM pollution situation.

Figure 7 represents the predicted results of PM ambient contributions in the receptor area under the upgrading of the China III to China V emission standards, as determined by RSM-PM_HSS9-300. It shows that the PM ambient concentrations in Beijing decreased slightly under the upgrade from the China III to China V emission standards. However, the degree of reduction varied across different regions of Beijing. The drop of PM concentrations was more significant in relatively heavily polluted areas, indicating that PM in highly polluted areas is more sensitive to changes in emission standards than in other areas. Specifically, the PM concentration under the China III (baseline scenario) was 64.12 μg/m³, while that under the China IV and China V emission standards (control scenario), it dropped to 48.23 and 38.60 μg/m³, respectively. This result aligns with the environmental monitoring data provided by the Beijing Ecology and Environment Bulletin (BMEEB), which indicates that the annual average concentration of $PM_{2.5}$ in Beijing decreased from 84.11 μg/m³ in 2014 to 43.07 μg/m³ in 2019. This trend supports our study's assessment of the environmental benefits of tightening vehicle emission standards on reducing particulate matter concentration, thereby corroborating the credibility of our findings.

Figure 8 displays the contribution of three precursor pollutants from vehicle emissions (NOx, VOCs, and primary PM) to the reduction of PM concentrations in Beijing under the China III, China IV, and China V emission standards, using

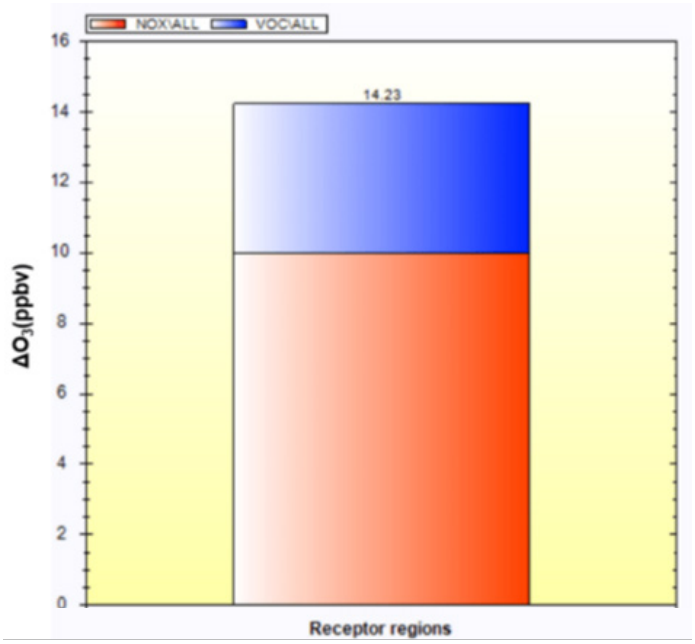

(a) China III ~ China IV

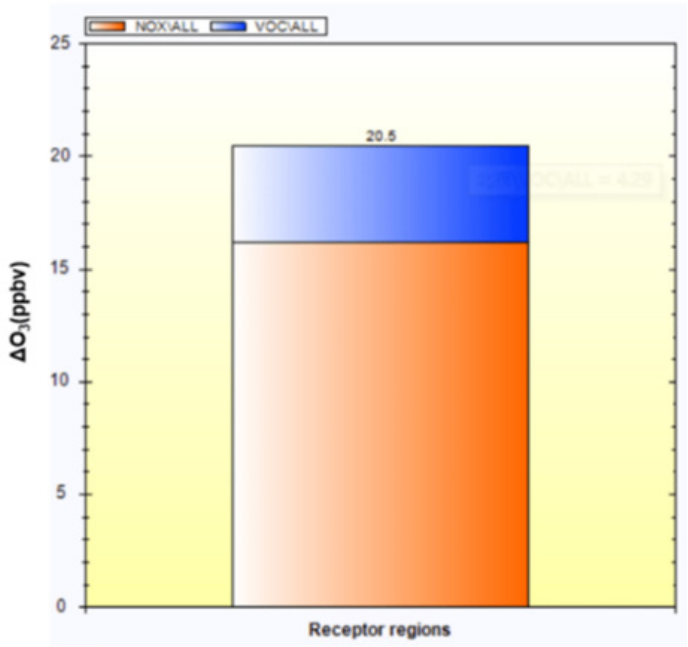

(b) China III ~ China V

Figure 6. Contribution of O_3 concentration reduction across different emission standard upgrade ranges

the source distribution function of RSM-VAT. The stacked bar plots, with three different colors, represent the proportions of primary PM, NOx, and VOCs in the reduction of PM concentration, with the vertical axis showing the reduction of PM concentration (ΔPM in μg/m³). The baseline scenario uses the China III emission standard, while the control scenarios use the China IV and China V, respectively.

The results show that primary PM plays a dominant role in reducing particulate matter concentration in Beijing, contributing significantly to the overall reduction, aligning with the findings reported by Pan et al. (2020). However, NOx exhibits a 'negative reduction' control effect, meaning that reducing NOx emissions does not always positively impact

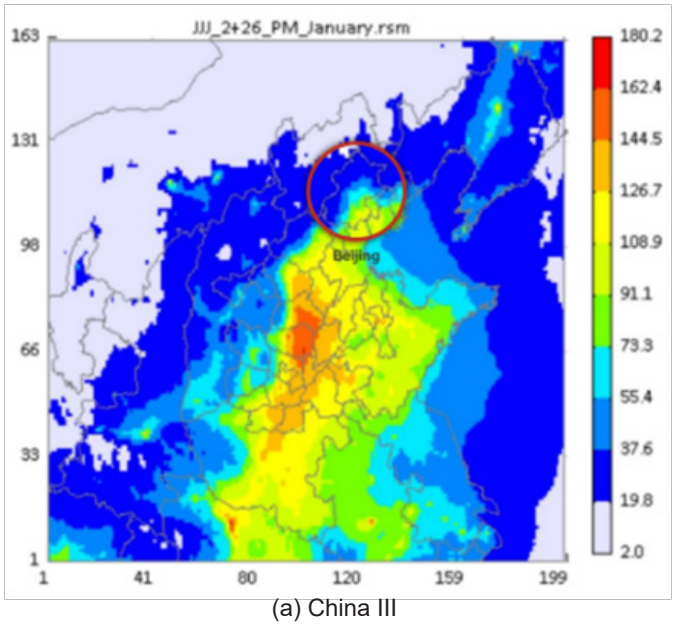

(a) China III

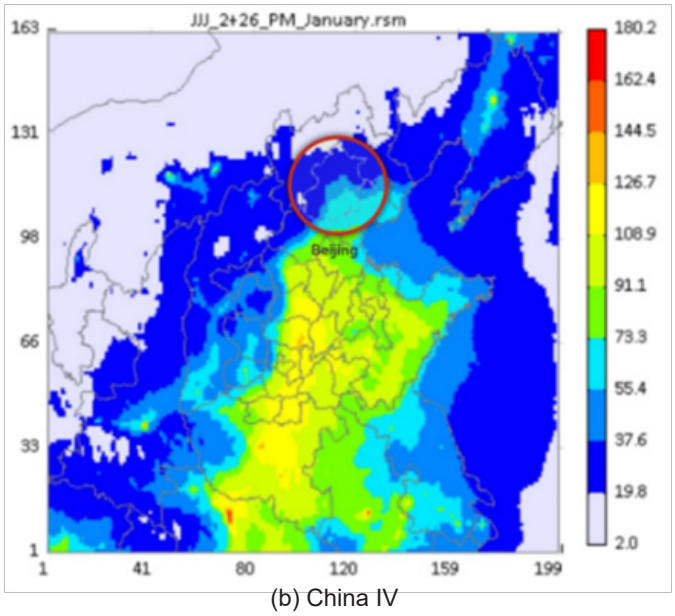

(b) China IV

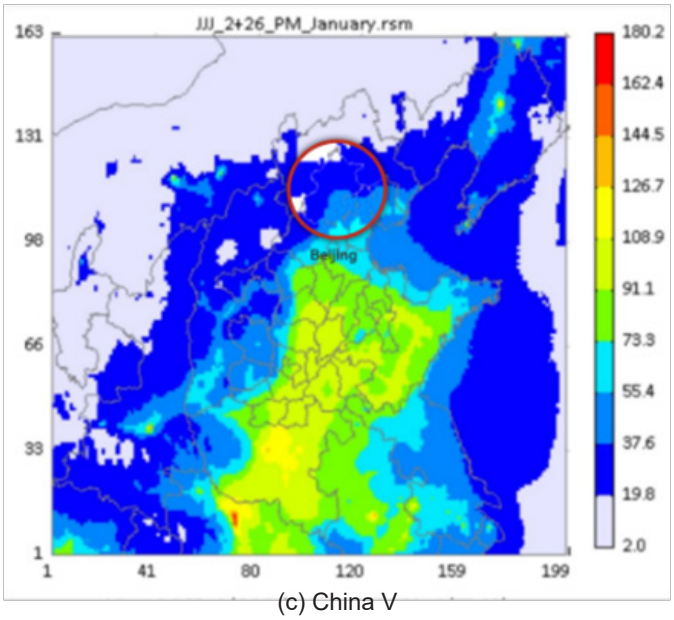

(c) China V

Figure 7. Two-dimensional distribution of primary PM concentration under different emission standard

PM concentration reduction. In some cases, it may actually lead to an increase in PM concentration. Studies have shown that the fundamental reason for this negative impact is the 'titration effects' of the NO component in NOx (Akimoto et al., 2022; Dai et al., 2024). NO reacts with O_3 in the atmosphere, consuming O_3 and resulting in a decrease in precursors that lead to PM formation (Tao et al., 2018; Brown et al., 2006). This negative contribution is particularly associated with low-lying pollution sources, such as vehicle exhaust emissions. Vehicles are one of the primary sources of NOx emissions in urban areas, which are typically more prone to PM pollution (Lv et al., 2020).

Therefore, excessive reduction of NOx emissions from vehicles, especially without additional measures to simultaneously control O_3 and other PM precursors, may inhibit PM control and reduction. Overall, developing pollution control strategies for both O_3 and PM requires considering the complex interactions and impacts among pollutants and their precursors. Simply reducing emissions of a single pollutant may not be sufficient to achieve the goal of reducing overall pollution levels.

Implications

During the transition from the China III to China V emission standards, the Chinese government achieved significant environmental benefits. Nevertheless, China's emission standards still trail behind those of Europe and the United States, indicating ample room for further emissions reduction. In the Beijing-Tianjin-Hebei region, measures such as vehicle purchase restrictions, usage limitations, and the promotion of new energy vehicles were implemented during this transition period. Additionally, outdated vehicles that failed to meet emission standards were mandatorily scrapped to optimize the vehicle fleet structure. For example, in Beijing, from 2009 to 2019, a total of 2.95 million outdated vehicles were decommissioned, significantly enhancing the vehicle fleet composition. Furthermore, the Chinese government upgraded fuel standards multiple times. In 2010, the limits for sulfur, olefin, and manganese content in gasoline were set at 150 μg/g, 30%, and 16 mg/L, respectively. By 2019, these limits were reduced to 10 μg/g, 18%, and 2 mg/L, respectively, resulting in decreased pollutant emissions. In 2019, emissions of the four major pollutants from motor vehicles (CO, VOCs, NOx, $PM_{2.5}$) decreased by 70%, 78%, 51%, and 73%, respectively, compared to 2009 (Wu et al., 2023).

Efforts for balanced and coordinated development in the Beijing-Tianjin-Hebei region have impacted pollutant and greenhouse gas emissions. Coordinated emission reduction measures and environmental governance policies led to a year-on-year decrease in pollutant concentrations ($PM_{2.5}$, NO_2, SO_2, O_3) at monitoring stations in the region from 2016 to 2020, signifying an improvement in urban environmental quality (Ding et al., 2023). The authors suggest that while rigorously tightening vehicle emission standards, future government policies should also prioritize promoting new energy vehicles, adopting cleaner fuels, and timely decommissioning outdated vehicles. These measures will contribute to reducing pollutant concentrations in the atmospheric environment of the Beijing-Tianjin-Hebei region.

Conclusions

This study evaluated the environmental improvement from the China III to China V emission standards by inputting real tested emission data and background data into the RSM to obtain O_3 and PM ambient concentrations in Beijing.

Our results show that the upgrade of emission standards led to a decrease of NOx, VOCs, and primary PM, which are precursors of O_3 and PM from vehicle emission. From our tests, the emission factors for NOx, VOCs and primary PM from gasoline vehicles under the China III emission standards are 206.42 mg/km, 233.12 mg/km, and 6.00 mg/km, respectively. Under the China IV and V emission standards, these factors are reduced to 88.53 mg/km, 84.98 mg/km, 3.60 mg/km and 27.88 mg/km, 42.88 mg/km, 1.91 mg/km, respectively. For diesel vehicles, the emission factors for NOx, VOCs and primary PM under the China III emission standards are 7976.71 mg/km, 811.95 mg/km, 63.77 mg/km, respectively. Under the China IV and V emission standards, these factors decrease to 5224.06 mg/km, 516.77 mg/km, 33.22 mg/km, and 4846.96 mg/km, 472.77 mg/km, 14.42 mg/km, respectively.

Furthermore, the corresponding RSM output results show that the ambient concentrations of O_3 and PM have significantly decreased. O_3 concentrations dropped from 92.70 ppbv to 78.47 ppbv and 72.20 ppbv, while PM concentrations decreased from 64.12 μg/m³ to 48.23 μg/m³ and 38.60 μg/m³, respectively. The environmental benefits achieved from the China III to China IV standards were greater than those from China IV to China V. Regarding O_3 and PM precursors (NOx, VOCs, Primary PM), NOx plays a pivotal role in reducing O_3 concentrations, whereas primary PM is the foremost factor in mitigating PM concentrations.

The accuracy and consistency of the RSM model with actual monitoring data are reflected in the PM response results. However, the O_3 response results based on vehicle exhaust appear somewhat idealized compared to actual environmental concentrations. Future research could enhance the RSM design or integrate additional methods to improve the prediction and evaluation of ozone concentrations. Additionally, future studies should include the China VI emission standards to assess the environmental benefits of stricter vehicle emission standards over a longer time span. Furthermore, exploring other pollutants, such as secondary organic aerosols (SOA), could provide a more comprehensive understanding of environmental benefits.

Finally, in addition to continuing to tighten emission standards for motor vehicles, the government should adopt a multi-faceted approach. This includes improving the structure of the motor vehicle fleet, promoting the use of new energy vehicles, and ensuring coordinated development in the Beijing-Tianjin-Hebei region, among other measures, to reduce pollutant emissions through various strategies.

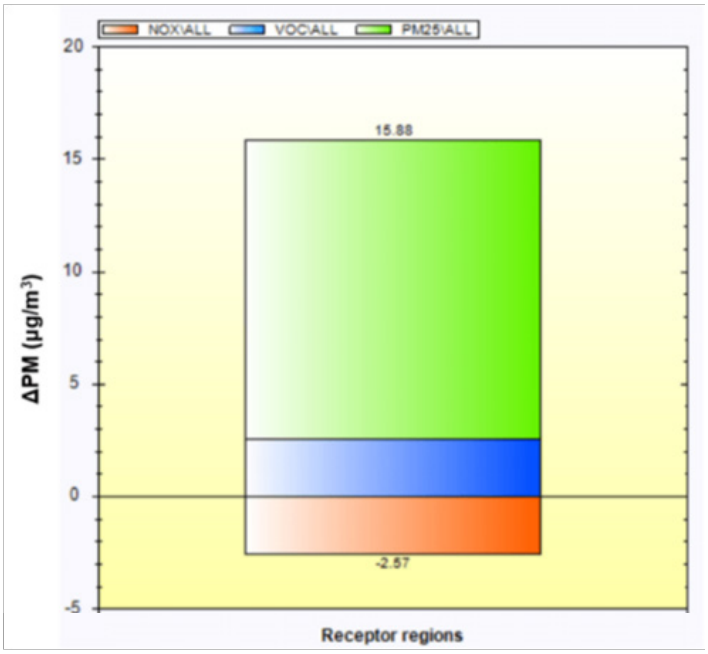

(a) China III ~ China IV

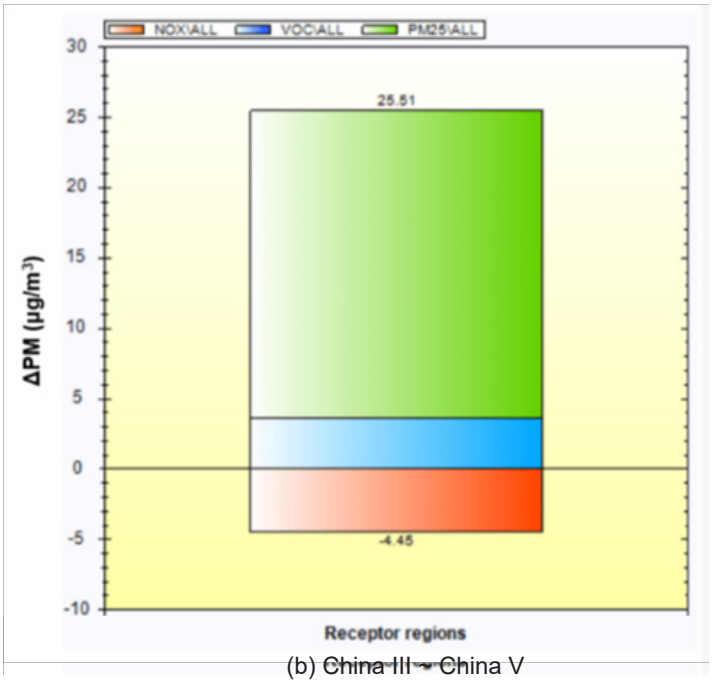

(b) China III ~ China V

Figure 8. Contribution of primary PM concentration reduction across different emission standard upgrade ranges

Acknowledgement

This study was sponsored by the National Key Research and Development Program of China (2022YFC3703600), and International Clean Energy Talent Program 2017 of China Scholarship Council (201702660024).

References

Aelion, C.M., Davis, H.T, Liu, Y., Lawson, A.B. & McDermott, S. (2009). Validation of Bayesian kriging of arsenic, chromium, lead, and mercury surface soil concentrations based on internode sampling. *Environmental Science & Technology,*43(12).

Akimoto, H. & Tanimoto, H. (2022). Rethinking of the adverse effects of NOx-control on the reduction of methane and tropospheric ozone–Challenges toward a denitrified society. *Atmospheric Environment*, 277: 119033. DOI:10.1016/j.atmosenv.2022.119033

BMEEB (2022). Beijing Ecology and Environment Statement 2021, http://sthjj.beijing.gov.cn/bjhrb/index/xxgk69/sthjlyzwg/1718880/1718881/1718882/325831146/2022122313533794930.pdf.

Box, G.E.P. & Draper, N. (2007). Response Surfaces, Mixtures, and Ridge Analyses, Second Edition of Empirical Model-Building and Response Surfaces, 1987, Wiley.

Brown, S.S., Ryerson, T.B., Wollny, A.G., Brock, C.A., Peltier, R., Sullivan, A.P., Weber, R.J., Dubé, W.P., Trainer, M., Meagher, J.F., Fehsenfeld, F.C. & Ravishankara, A.R. (2006). Variability in nocturnal nitrogen oxide processing and its role in regional air quality. *Science*, 311(5757), pp. 67-70. DOI:10.1126/science.1120120.

Daellenbach, K.R., Uzu, G., Jiang J., Cassagnes, L.E., Leni, Z., Vlachou, A., Stefenelli, A., Canonaco, F., Weber, S., Segers., A., Kuenen, J.P.J., Schaap, M., Favez, O., Albinet, A., Aksoyoglu, S., Dommen, J., Baltensperger, U., Geiser, M., Haddad, E. I., Jaffrezo, J.L & Prévôt, S.H.A. (2020). Sources of particulate-matter air pollution and its oxidative potential in Europe. *Nature*, 587(7834), pp. 414-419. DOI:10.1038/s41586-020-2902-8.

Dai H.B., Liao, H., Wang, Y. & Qian, J. (2024). Co-occurrence of ozone and PM2.5 pollution in urban/non-urban areas in eastern China from 2013 to 2020: Roles of meteorology and anthropogenic emissions. *Science of The Total Environment*, 924, 171687. DOI:10.1016/j.scitotenv.2024.171687.

Deng, T., Huang, Y.Q., Li, Z.N., Wang, N., Wang, S.Q., Zou, Y., Yin, C.Q. & Fan. S.J. (2018). Numerical simulations for the sources apportionment and control strategies of PM 2.5 over Pearl River Delta, China, part II: Vertical distribution and emission reduction strategies. *Science of the Total Environment*, 634. DOI:10.1016/j.scitotenv.2018.04.209.

Ding, W & Shuhua, L. (2023). Impact assessment of air pollutants and greenhouse gases on urban heat wave events in the Beijing-Tianjin-Hebei region. *Environmental Geochemistry and Health*, 45(11): pp. 7693-7709. DOI:10.1007/s10653-023-01677-7.

Guha, A.K. & Gokhale, S. (2023). Urban workers' cardiovascular health due to exposure to traffic-originated PM2.5 and noise pollution in different microenvironments. *Science of the Total Environment*, 859, 160268. DOI:10.1016/j.scitotenv.2022.160268.

Hammersley, J. (1960). Monte Carlo methods for solving multivariable problems. *Proceedings of the New York Academy of Science*, 86: pp. 844-874. DOI:10.1111/j.1749-6632.1960.tb42846.x.

Jia, X., Wang, S.X., Jang, C., Zhu, Y., Zhao, B., Ding, D., Wang, J.D., Zhao, L.J., Xie, H.X. & Hao, J.M. (2017). ABaCAS: an overview of the air pollution control cost-benefit and attainment assessment system and its application in China. *The Magazine for Environmental Managers–Air & Waste Management Association*, (April). https://www.abacas-dss.com/Files/paper/ABaCAS_EM_April_2017_xing.pdf.

Kumar, P.G., Lekhana, P., Tejaswi, M. & Chandrakala, S. (2021). Effects of vehicular emissions on the urban environment-a state of the art. *Materials Today: Proceedings*, 45: pp. 6314-6320. DOI: 10.1016/j.matpr.2020.10.739.

Lao, Y. W., Zhu, Y., Jang, C., Lin, C. J., Xing, J.,Chen, Z. R., Xie, J. P., Wang, S. X. & Fu, J. (2012). Research and development of auxiliary decision tools for regional air pollution control based on response surface mode. *Journal of Environmental Sciences*, 32(08), pp. 1913-1922. DOI:10.13671/j.hjkxxb.2012.08.019. (In Chinese)

Latha, R., Shahana, B., Dolly, M., Rupal, A., Trina, M., Priyadarshi, M. & Murthy, B.S. (2023). On the transition of major pollutant and O3 production regime during Covid-19 lockdowns. *Journal of Environmental Management*, 328, 116907. DOI:10.1016/j.jenvman.2022.116907.

Liu, C. & Shi, K. (2021). A review on methodology in O3-NOx-VOC sensitivity study. *Environmental Pollution*, 291, 118249. DOI:10.1016/j.envpol.2021.118249.

Liu, F., Zhu, Y. & Zhao, Y. (2008). Contribution of motor vehicle emissions to surface ozone in urban areas: A case study in Beijing. *The International Journal of Sustainable Development & World Ecology*, 15(4), pp. 345-349. DOI:10.3843/SusDev.15.4:9.

Lv, Z.F., Wang, X.T., Deng, F.Y., Ying, Q., Archibald, T.A., Jones, J.R., Ding, Y., Cheng, Y., Fu, M.L., Liu, Y., Man, H.Y., Xue, Z.G., He, K.B., Hao, J.M. & Liu, H. (2020). Source–receptor relationship revealed by the halted traffic and aggravated haze in Beijing during the COVID-19 lockdown. *Environmental science & technology*, 54(24), pp, 15660-15670. DOI:10.1021/acs.est.0c04941.

Lyu, M., Bao, X.F., Zhu, R.C. & Matthews, R. (2020). State-of-the-art outlook for light-duty vehicle emission control standards and technologies in China. *Clean Technologies and Environmental Policy*, 22(4), pp. 757-771. DOI:10.1007/s10098-020-01834-x.

Ministry of Ecology and Environment of the People's Republic of China (MEE). (2022) https://www.mee.gov.cn. Last access: 20 August 2022.

Ministry of Ecology and Environment of the People's Republic of China (MEE). (2023) https://www.mee.gov.cn. Last access: 1 August 2023.

Nguyen, K. & Dabdub, D. (2022). NOx and VOC control and its effects on the formation of aerosols. *Aerosol Science & Technology*, 36(5), pp. 560-572. DOI:10.1080/02786820252883801.

Pan, Y. Z. (2020). Improvement and application of PM2.5 source contribution analysis Method based on Response Surface model technique. *South China University of Technology,* DOI:10.27151/d.cnki.ghnlu.2020.002204. (in Chinese)

The People's Government of Beijing Municipality (PGBM). (2021) http://www.beijing.gov.cn. Last access: 1 August 2021.

Wang, Y.H., Gao, W.K., Wang, S., Song, T., Gong, Z.Y., Ji, D.S., Wang L.L., Liu, Z.R.,Tang, G.Q., Huo, Y.F., Tian, S.L., Li, J.Y., Li, M.G., Yang,Y., Chu, B.W., Petaja, T., Kerminen, V.M., He, H., Hao, J.M., Kulmala, M., Wang, Y.S. & Zhang, Y.H. (2020). Contrasting trends of PM2.5 and surface-ozone concentrations in China from 2013 to 2017. *National Science Review*, 7(8), pp. 1331-1339. DOI:10.1093/nsr/nwaa032.

Wu, T.R., Cui, Y.Y., Lian, A.P., Tian, Y., Li, R.F., Liu, X.Y., Jing, Y., Xue, Y.F., Liu, H. & Wu, B.B. (2023). Vehicle emissions of primary air pollutants from 2009 to 2019 and projection for the 14th Five-Year Plan period in Beijing, China. *Journal of Environmental Sciences*, 124(02), pp. 513-521. DOI:10.1016/j.jes.2021.11.038.

Xing, J. (2011). Study on non-linear response relationship between air pollution emissions and environmental effects. *Tsinghua University*, https://kns.cnki.net/kcms2/article/abstract?v=4wkQyjAcIEdPh2Yz1dvthqvcfOngyxm32aJgNvaSA4efiNy_bMJJ4XlzsbKsiQczmoIqt74U_xNLfCgwd3hxR2AIh1OI7XMyf76pbtSLWw1Dubs4VmUGJvvJ6fLOGwKrwODdmuqlysGVyPacwW_Mt7j_RMJXR2h75EvN8sWktx0_lBW-P2WMKiacY0eic2ET&uniplatform=NZKPT&language=CHS. (In Chinese)

Xu, J., Xu, X.B., Lin, W.L., Ma, Z.Q., Ma, J.Z., Wang, R., Wang, Y., Zhang, G. & Xu, W.Y. (2020). Understanding the formation of high-ozone episodes at Raoyang, a rural site in the north China plain. *Atmospheric Environment*, 240, 117797. DOI:10.1016/j.atmosenv.2020.117797.

Xue, X.H. (2020). A brief discussion on the harm of photochemical smog and its control countermeasures. *Sichuan Environment*, (04), pp. 75-76+60. DOI:10.14034/j.cnki.schj.2000.04.025. (In Chinese)

Zhang, Q.J., Liu, J.Y., Wei, N., Song, C.B., Peng, J.F., Wu, L. & Mao, H.J. (2023). Identify the contribution of vehicle non-exhaust emissions: a single particle aerosol mass spectrometer test case at typical road environment. *Frontiers of Environmental Science & Engineering*, 17(5), 62. DOI:10.1007/s11783-023-1662-8.

Zhao, B., Wang, S.X., Dong, X.Y., Wang, J.D., Duan, L., Fu, X., Hao, J.M. & Fu, J.S. (2013a). Environmental effects of the recent emission changes in China: implications for particulate matter pollution and soil acidification. *Environmental Research Letters*, 8(2), 024031. DOI:10.1088/1748-9326/8/2/024031.

Zhao, B., Wang, S.X, Wang, J.D., Fu, S.J., Liu, T.H., Hua, J.Y., Fu, X. & Hao, J.M. (2013b). Impact of national NOx and SO2 control policies on particulate matter pollution in China. *Atmospheric Environment*, 77, pp. 453-463. DOI:10.1016/j.atmosenv.2013.05.012.